GEOPHYSICAL RESEARCH LETTERS, VOL. 26, NO. 19, PAGES 2945-2948, OCTOBER 1, 1999

Interannual Variations of Global UV Radiation in Santiago, Chile (33.5°S)

Sergio Cabrera[1] and Humberto A. Fuenzalida[2]

Universidad de Chile, Santiago

Abstract Observations with a four-channel UV radiometer in Santiago, Chile (33.5°S, 70.6°W) from January 1992 to December 1998 are presented. Channels are centered at 305, 320, 340 and 380 nm with a 10 nm bandwidth. Measurements were made at one-minute intervals. Hourly mean values at noon for 305 and 340 nm are presented as well as instantaneous irradiances for 60° of solar zenith angle. Their aperiodic variations on a seasonal scale are discussed with respect to the quasi-biennial oscillation (QBO) and ENSO phenomena. A significant positive trend that must be caused by decreasing total ozone is found in 305 nm irradiance. On a seasonal basis, this negative trend appears strong and significant during winter.

Introduction

Negative global trends in stratospheric ozone are associated with an increase of solar UV-B radiation at the surface of the earth as documented in data taken with spectroradiometers in austral South America (Diaz et al., 1994; Bojkov et al., 1995) and elsewhere (McKenzie et al., 1991; Kerr and McElroy, 1993; Zerefos et al., 1997).

Global solar UV irradiance in Santiago was observed with a four-channel UV radiometer. This radiometer facilitates simultaneous measurements at a set of wavelengths with moderate spectral resolution at time intervals as short as one second. In order to infer a UV spectrum from the four voltages at least two methods have been recently proposed (Dahlback, 1996, and Fuenzalida, 1998).

Seven years of data may be short for a significant evaluation of trends but are informative of interannual variability and can be considered a first step towards a local UV climatology. The springtime record at latitude 33.5°S, is marginally affected by the Antarctic ozone depletion but the summer regime may receive the influence of ozone-poor air masses drifting towards mid-latitudes after the polar vortex has broken up, as observed by Roy et al. (1990) over Australia and by Kirchhoff et al. (1996) in South America.

Santiago is located in the western foothills of the Andes, about 100 km from the Pacific Ocean. Its altitude increases from 540 to 700 m above sea level within a fairly closed basin. It is situated at the eastern margin of a subtropical anticyclone beneath a subsidence inversion and with weak prevailing winds. Its climate is semi-arid with most of the 300 mm of annual rain falling from May to September. Summer is very dry and cloudless while in winter cloud cover is variable with a few active fronts passing over. The city, hosting about 5 million people, suffers from heavily polluted air. Meteorological conditions favor a large concentration of particles in the air during fall and winter, but urban ozone is more abundant during summer. Central Chile is affected by ENSO phenomena with El Niño years associated with rainy winters, and with dry La Niña years (Montecinos et al., 1999). Included in the UV record is the rainy winter of 1997, when a strong El Niño was in progress. On the other extreme is the 1998 drought, during which La Niña conditions prevailed.

Data and methodology

Since 1992 a four-channel UV radiometer has been in operation in Santiago, Chile (33° 28'S, 70°38'W). The radiometer, manufactured by BSI[1] is of a portable type (PUV-510), with no temperature control. Filters and corresponding photodiodes are arranged under a teflon diffuser. The four UV channels have a bandwidth of approximately 10 nm each and are centered at nominal wavelengths of 305, 320, 340 and 380 nm.

The instrument was calibrated six times during the seven-year period; details are listed in Table 1. The calibration constant, k, is defined as the ratio between the voltage increment and the convolution sum of relative responsivity and the light source spectrum, as stated in equation 1 below, (Dahlback, 1996). Its value was determined using responsivity values inferred from the instrument catalog and data for similar radiometers (GUV). A straight line was fitted by least squares to all reliable calibrations and k values were interpolated for each month. Largest deviations from the fitted line expressed as absolute value were 3, 8, 7 and 4% in channels 305, 320, 340 and 380 nm, respectively.

Voltages from the four UV channels were fed into a computer program which, after reduction to a fixed temperature (25°C) following BSI 1998 recommendations, retrieved the full spectrum from 280 to 400 nm with one nanometer resolution by a constrained inversion method (Fuenzalida, 1998). Basically each channel voltage can be expressed as

$$\Delta V_i = k_i \sum_j R'_{ij} E_j \qquad (1)$$

where index $i = 1, 2, 3, 4$ indicates channel number and index j specifies wavelength. Here E stands for monochromatic

[1] S. Cabrera is with the Instituto de Ciencias Biomédicas, Facultad de Medicina, Universidad de Chile, Casilla 70061-7, Santiago, Chile, (e-mail: *scabrera@machi med.uchile cl).*

[2] H.A. Fuenzalida is with the Departamento de Geofísica, Facultad de Ciencias Físicas y Matemáticas, Universidad de Chile, Casilla 2777, Santiago, Chile, (e-mail: *hfuenzal@dgf uchile cl).*

Paper number 1999GL010828.
0094-8276/99/1999GL010828$05.00

[1] : Biospherical Instruments Inc., San Diego, California.

Table 1: Calibration details.

Date	Reference	k *			
		305 nm	320 nm	340 nm	380 nm
Jan, 92	Lamp	1.4166	0.0349	0.0425	0.0097
Jun, 93	Lamp	1.3978	0.0528	0.0448	0.0099
May, 94#	Lamp	1.3466	0.1368	0.0339	0.0453
Apr, 96@	Ref. GUV	1.5559	0.1250	0.0282	0.0460
Oct, 98	SUV-100	1.4779	-	0.0269	-
Jan, 99	SUV-100	1.4947	0.1261	0.0256	0.0499

(*): Negative voltages are measured in channels 320, 340 and 380, but k's sign has been omitted.
(#): Photodiode of channel 320 was changed and sensitivities of channels 320 and 380 were modified.
(@): Partially cloudy

irradiance and R' for channel responsivity. From these four integral relations a smoothed version of $E(\lambda)$ is obtained by constrained inversion (Schanda, 1986) to which the fine structure of extraterrestrial solar spectrum, properly scaled, is added. With reference to a scanning radiometer the uncertainty of the retrieved irradiance at 305 nm is less than 12 % for solar zenith angle up to 55°.

Daily files with one measurement per minute were processed to produce an average over a one-hour interval centered at solar noon. Also, in order to avoid the large annual cycle, irradiance, recorded at 60° of solar zenith angle (SZA), was extracted from daily files. A comparison between morning and afternoon values showed non-significant differences in 305 and 340 nm irradiances and because ozone is only determined once a day both daily values were averaged. Since cloudiness and total ozone have annual cycles the resulting irradiance series still exhibits a small annual variation. The remaining periodic component was suppressed by subtraction of the mean cycle. Mean seasonal anomalies were computed as three-month averages with summer starting in December.

Variations of 305 nm irradiance, reaching the ground level at SZA=60°, depend on ozone absorption and scattering by particles (including clouds). TOMS ozone data over Santiago are incomplete, since there is a gap from the end of November, 1994, to August, 1996 and no ground-based observations exist in its surroundings. Total ozone inferred as suggested by Stamnes et al (1991) correlated poorly against TOMS data, the main difference being a larger annual cycle and smaller values in the low-sun season. For this reason the incomplete TOMS record was used although in a particular manner explained below.

For wavelengths longer than 320 nm, the main controlling variable is cloud, cover and type, and aerosols as a secondary factor. Independent information can be gathered from satellite data but their use is hindered due to a reduced sensitivity for particle matter in the atmospheric boundary layer and its low space resolution. Cloud and aerosol attenuation can be inferred from either the 340 nm or 380 nm irradiance since at these wavelengths ozone absorption is negligible. Hereafter, ozone will be taken from TOMS, but 340 nm irradiance will be instrumental in characterizing atmospheric transmission.

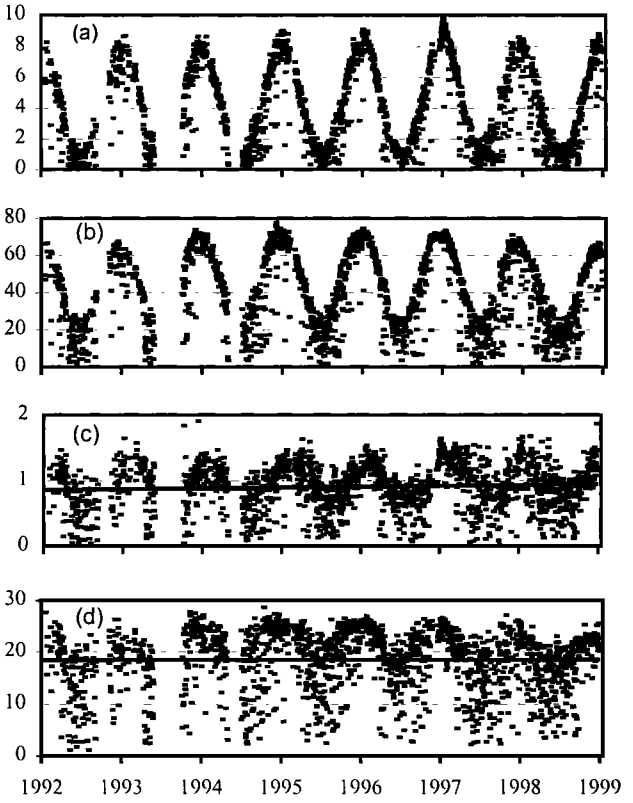

Figure 1: Hourly mean irradiance in Santiago (33.5°S) at solar noon: (a) 305 nm and (b) 340 nm. Instantaneous irradiance observed at SZA=60°: (c) 305 nm, and (d) 340 nm,.All expressed in $\mu W/cm^2/nm$. On the horizontal axis labels and ticks indicate Jan 01 of each year. Linear trends in (c) and (d) correspond to 14.7 and 1.6 % per decade, respectively.

Results

Figure 1 presents monochromatic irradiances at 305 nm and 340 nm averaged over a one-hour interval centered at solar noon. The annual cycle spans from 1 to 9 $\mu W/cm^2/nm$ at 305

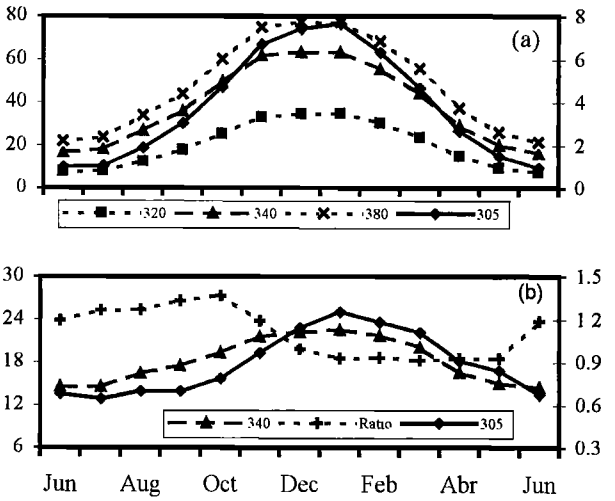

Figure 2: Monthly mean irradiance in Santiago (33.5°S):
(a) At noon, 305 (solid line, right axis), 320, 340 and 380 nm (left axis). (b) At SZA=60°, 305 (solid line, right axis), 340 and ratio 340/380 (left axis). Irradiance units are $\mu W/cm^2/nm$.

nm and from 25 to 75 μW/cm^2/nm at 340 nm, approximately. The large annual cycle, mostly due to the SZA variations, can be suppressed when irradiances only at SZA=60° are plotted (same Figure 1). Here the annual variation at 340 nm must be mostly due to changes in cloud cover while at 305 nm the ozone depth influence must also be accounted for. Linear trends for both wavelengths are positive amounting to 0.14 and 0.29 μW/cm^2/nm in a decade in 305 nm and 340 nm, respectively.

Monthly averages of the noon hourly mean are shown in Figure 2 where the 305 nm line exhibits an asymmetry with respect to the summer solstice (December) due to the ozone annual cycle that runs high in winter and spring and low during summer and fall. This can be verified in the lower part of Figure 2 where monthly means of daily irradiances at 305 nm and 340 nm observed at SZA=60° are presented together with their ratio, which is responsive to total ozone. When these annual cycles are taken from the monthly record at SZA=60°, time series for anomalies are obtained, as shown in Figure 3. This figure indicates that 305 nm irradiance, E_{305}, has been increasing; while at 340 nm the irradiance exhibits no apparent trend over the whole period. As a consequence the ratio, E_{340}/E_{305}, decreased implying a negative trend for ozone. This trend cannot be verified with TOMS data which, as commented above, is too patchy. A linear correlation between TOMS data and 340/305 ratio over Santiago, is rather low, accounting for 55% of the variance. However, by forcing an expression like equation 2 the fraction of explained variance increases up to 90% showing that a better fitting can be attained with this exponential dependence.

Discussion

A comparison between the upper and central parts of Figure 3 reveals that most of the rapid fluctuations in 305 nm follow those in 340 nm, so that changes in monthly cloud cover determine variations in UV-B radiation. However, the positive trend in 305 nm irradiance is not reproduced by the 340 nm trace, which grows at a slower pace forcing a negative trend in the E_{340}/E_{305} ratio.

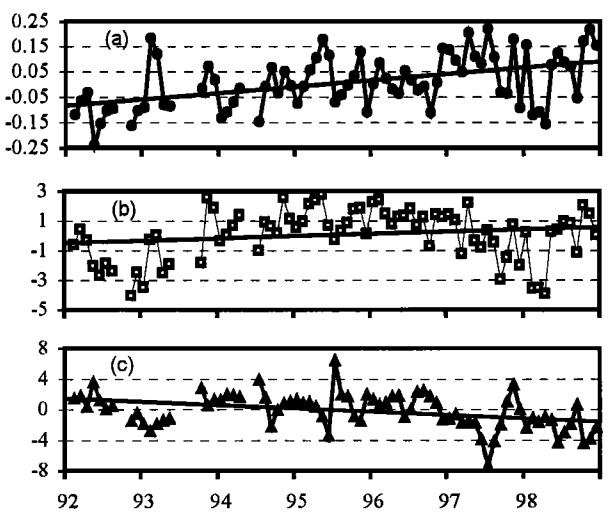

Figure 3: Monthly mean anomaly of irradiance observed at SZA=60°: (a) 305 nm, (b) 340 nm and (c) their ratio 340/305. Trends are shown by least squares lines. Irradiance units are μW/cm^2/nm. On the horizontal axis labels and ticks indicate Jan 01 of each year.

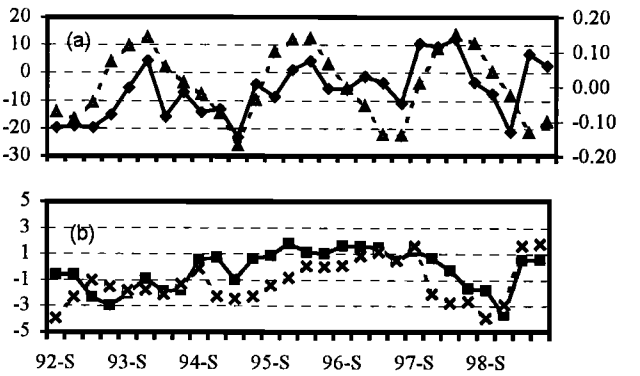

Figure 4: (a) Seasonal mean anomaly of irradiance at SZA=60° and 305 nm (solid line, right axis) and QBO at 30 hPa in m/s (dashed line, left axis). (b) Seasonal mean anomaly of irradiance at SZA=60° and 340 nm (solid line) and Southern Oscillation Index (dashed line). On the horizontal axis summer (S: Dec-Jan-Feb) seasons are indicated.

In an attempt to relate ozone from TOMS to noon irradiance observations on a daily basis, an atmospheric transmission was defined as $\tau = E_{340}$ (observed)/E_{340} (model). Here E_{340} (model) is obtained with Stamnes et al. (1988) discrete ordinate code for a Rayleigh atmosphere with a standard temperature profile, so that $0 < \tau < 1$. An empirical relation explaining a 90% of the variance of hourly averages at noon is then

$$E_{305} = A\,\tau\,\exp\{-m\,\Omega / \cos Z\} \qquad (2)$$

Here, Ω is total ozone, Z is the SZA; A and m are empirical constants obtained in the fitting process.

The relation between ozone and the quasi-biennial oscillation (QBO) can be explored in Santiago's 305 nm observations. At 33.5°S the site is on the poleward side of the phase change latitude found by Hasebe (1983) so that the westerly phase of the QBO will favor low ozone (high UV-B) over Santiago. On a seasonal basis the QBO at 30 hPa and 305 nm irradiance are shown in Fig. 4-a from which an approximate phase agreement is apparent. A second interannual mechanism affecting Santiago's UV regime is ENSO. In Figure 4-b a seasonal plot of the Southern Oscillation Index (SOI) is shown together with the 340 nm irradiance. In this case the controlling factor is cloudiness and although the relation is rather loose both traces are clearly in phase except for the first year and a half. This occurred when aerosols from Mount Pinatubo eruption (or Hudson's) were still in the stratosphere. The 1997-8 ENSO came associated with an unusually cloudy summer that produced profound dips in both 305 and 340 nm irradiances. (Also apparent in Figure 1 from the number of scattered points inside the envelope depicted by clear days).

To evaluate irradiance trends only observations taken at SZA=60° were used and reduced to decadal fractional changes. For the complete set of daily values of irradiance at 305 nm, shown in Figure 1-c, a least squares fitted linear trend and its 95% confidence interval are (3.83±2.26)*10^{-5} μW/cm^2/nm per day, so that a significant positive trend exists in the UV-B range. Irradiance at 305 nm and SZA=60° is

around 1 $\mu W/cm^2/nm$ so the trend represents a decadal increase of (14.7±8.7)%. For 340 nm irradiance the linear trend and its 95% confidence interval are $(8.07\pm38.5)*10^{-5}$ $\mu W/cm^2/nm$ per day, indicating that no significant trend exists at this wavelength, the corresponding decadal increase would be (1.6±7.6)%.

When data are grouped in 77 monthly mean values and any annual cycle has been extracted, the anomalies shown in Figure 3 can also be subject to decadal trend estimation. The resulting increase at 305 nm is (21.2±13.0)% while at 340 nm is again not significant at the 95% level with (4.6±11.9)%. On a seasonal basis decadal trends for 305 nm were determined from 7 data points, one for each year. Only the winter trend resulted significant at the 95% level with a magnitude and confidence interval of (67.3±47.3)%, followed by spring, (19.3±20.8)%, and summer, (18.3±25.8)%, becoming non-significant in the fall (4.6±74.1)%. Therefore, most of the ozone loss happens in winter, suggesting a weaker meridional transport as a likely cause. The negative spring trend is barely non-significant. These rates of growth are similar to those evaluated by other authors. For instance, Zerefos et al. (1997), on the basis of seven years of data for Thessaloniki, Greece, at 40°N, found an increase of 27% per decade for 305 nm irradiance observed at SZA=63°. Also Gurney (1998) determined monthly trends for 305 nm at Point Barrow, Alaska, 60°N, from six years of deseasonalized data, finding positive trends from 30 to 100% per decade for most of the year but a decrease of 30% in June (boreal summer).

Equation 2, deduced from midday readings, is also valid at SZA=60°. In a differential form

$$\frac{dE_{305}}{E_{305}} = \frac{d\tau}{\tau} - \frac{m\ d\Omega}{\cos Z} \qquad (3)$$

relates fractional trends at 305 nm and 340 nm (through τ), to TOMS ozone. Since the fractional trend in E_{305} (0.147) is an order of magnitude larger than that of τ or E_{340} (0.016), the main responsible for the UV-B trend must be ozone. In order to explain the decadal UV-B growth, total ozone must decrease in around 11 DU, which corresponds to 3.7% depletion for an annual mean of 295 DU. The increment in 305 nm irradiance caused by this ozone decrease can be extended to midday conditions with due consideration of the change in SZA with season. For instance, in the summer and winter solstices the 11 DU imply decadal increments, in 305 nm irradiance, of 6.7% and 11.8% respectively, and a 7.9% in the equinoxes.

Hence, resting on the evidence furnished by seven years of data over Santiago, the decadal increase of 14.7% in 305 nm irradiance at SZA=60° is due in a 10% to clearer skies and in a 90% to ozone depletion. Therefore, although in a short time-scale the primary control of UV-B rests on cloudiness, in the long run it is ozone that exercises the decisive control.

In spite of the fact that these observations must be influenced by an acute local pollution condition, large-scale phenomena, as ENSO and QBO, have the prevailing control on UV radiation. Therefore, either air pollution has been a fairly constant factor or its impact is of second order in comparison with the large-scale factors.

Acknowledgments This research was supported by the Fondo Nacional de Ciencia y Tecnologia (FONDECYT) under Project # 1960734. Data before 1996 were collected under Project # 1143-91. The Inter-American Institute for Global Change Research (IAI) provided partial support through ISP2 Grant "A South-American Network for UV Measurements". TOMS data were taken from website of the Ozone Processing Team, NASA\Goddard Space Flight Center. Data on the QBO and SOI were taken from the Climate Prediction Center/NCEP-NOAA website.

References

Bojkov, R.D, V.E. Fioletov, and S. Diaz, The relationship between solar UV irradiance and total ozone from observations over southern Argentina, *Geophys. Res. Lett.* **22**(10):1249-1252, 1995

Dahlback, A. Measurements of biologically effective UV-doses, total ozone abundance and cloud effects with multi-channel moderate bandwidth filter instruments. *Appl. Opt.*, **35**, 6514-6521., 1996

Diaz,S.B., C.R.Booth,T.B.Lucas, and I. Smolskaia, Effects of ozone depletion on irradiances and biological dosis over Ushuaia. *Arch.Hydrobiol. Beih Ergebn. Limnol* **43**: 115-122, 1994

Fuenzalida, H., Global UV-spectra directly derived from observations with multichannel radiometers. *Appl Opt.*, **37**, 33: 7912-7919, 1998

Gurney, K.R Evidence for increasing ultraviolet irradiance at Point Barrow Alaska. *Geoph Res Lett.* **25**(6) 903-906 1998

Hasebe, F. Interannual variations of global total ozone revealed from Nimbus 4 BUV and ground-based observations, *J. Geophys. Res.*, **88**, 6819-6834, 1983.

Kerr,J.B. & C.T. McElroy Evidence for large Upward Trends of Ultraviolet-B Radiation linked to Ozone depletion. *Science*, ***262***: 1032-1034 1993

Kirchhoff, V., N.J. Schuch, D.K. Pinheiro and Joyce M. Harris, Evidence for an ozone hole perturbation at 30° South, *Atmospheric Environment*, **30**, 9, 1481-1488, 1996.

McKenzie,R.L, W.A. Mathews, and P.V. Johnston, The relationship between erythemal UV and ozone, derived from spectral irradiance measurements. *Geophys Res. Lett.,**18(12): 2269-2272. 1991***

Montecinos, A., A. Diaz and P. Aceituno, Seasonal diagnostic and predictability of rainfall in subtropical South America based on tropical Pacific SST, Accepted in *J of Climate*, 1999

Roy, C.T., H.P.Gies and E.Graime, Ozone depletion, *Science*, **347**, 235-236. 1990.

Schanda, E., Physical Fundamentals of Remote Sensing, *Springer-Verlag*, Berlin, 187 pp., 1986.

Stamnes, K., J. Slusser and M. Bowen. Derivation of total ozone abundance and cloud effects from spectral irradiance measurements. *Appl. Opt.*, **30**:30, 4418-4426 1991.

Stamnes, K., S.-C. Tsay, W.J. Wiscombe, and K. Jayaweera. Numerically stable algorithm for discrete-ordinate-method radiative transfer in multiple scattering and emitting layered media. *Appl Opt.*, **27**, 2502-2509 1988.

Zerefos, C.S., D.S. Balis, A.F. Bais, D. Gillotay, P.C. Simon, B. Mayer, and G. Seckmeyer, Variability of UV-B at four stations in Europe, *Geophys.Res.Lett.*, **24**(11),1363-1366, 1997.

(Received: May 26, 1999 Revised: July 29, 1999 Accepted: August 12, 1999)